

## Azimuth-angle-dependent reflectivity data from metallic gratings

A. P. HIBBINS, J. R. SAMBLES

Thin Film Photonics Group, Department of Physics, University of Exeter, Exeter EX4 4QL, England

and C. R. LAWRENCE

Defence Evaluation and Research Agency, Farnborough GU14 0LX, England

(Received 22 September 1997)

**Abstract.** In this work, we have used a new technique to characterize optically a periodically modulated metal–dielectric interface involving the measurement of the azimuthal-angle-dependent specular reflectivity. This method presents advantages over the conventional polar angle scan experiment since it requires no moving signal detector. The data recorded has been fitted to a conical version of Chandezon’s differential formalism using a single set of parameters describing the grating profile and metal permittivity. The fitted grating profile is in good agreement with the form found by the use of an atomic force microscope. This work therefore provides a new procedure for characterizing gratings as well as a convincing test of conical diffraction theory.

### 1. Introduction

It has long been known that the angle-dependent reflected radiation from a periodically modulated metal–dielectric interface (a metallic grating) may show intensity anomalies that are associated with the momentum-matching condition of a surface resonance [1–3]. This surface mode, the surface plasmon-polariton (SPP), is strongly localized at the metal–dielectric interface, consisting of a surface charge density oscillation and associated electromagnetic fields. Its momentum is greater than the maximum photon momentum available in the adjacent dielectric [4, 5]; so it cannot radiate from a flat metallic surface or be directly coupled to. However, we may couple to the mode using the wave-vector enhancement provided by a diffraction grating, the enhancement in the plane of the grating being in multiples of the grating wave-vector. Hence, by varying the angle of incidence of a monochromatic beam, we find specific angles at which we may couple resonantly to the SPP mode.

Experimentally, the excitation of the SPP is observed as a dip in the angle-dependent reflectivity of the incoming radiation. Researchers have used the differential formalism of Chandezon *et al.* [6] to model rigorously the in-plane reflectivity for a corrugated surface as a function of the polar angle of incidence. By varying the grating parameters used to generate such a theoretical trace, it is possible to obtain an excellent fit to the experimental data and hence determine the shape [7] and optical permittivity [8] of the metallic surface.

However, we do not have to be constrained to the in-plane geometry that is often used. Recent developments to Chandezon's original theory have permitted the modelling of systems where the Bragg vector of the grating is not in the plane of incidence [9]. The angle between the plane of incidence and the grating vector, we call the azimuthal angle  $\varphi$ . The grating is said to be in the conical mount when  $\varphi \neq 0$ . In this geometry, polarization conversion is induced [10] and, as a result, the reflectivity features have an increased sensitivity to the profile of the grating surface. Watts *et al.* [11] have successfully demonstrated that a surface may be confidently characterized using angle-dependent fits to reflectivity recorded for different azimuths.

All previous studies have used a fixed plane of incidence, varying the angle of incidence  $\theta$ . Here we use a new technique instead where we record the reflectivity data as a function of the azimuthal angle for a fixed angle of incidence. The great advantage of this procedure is that only the grating has to be rotated whilst the source and detector remain fixed.

The system chosen to study this new technique and to test the conical diffraction model is a periodically modulated gold-air interface. Experimental reflectivities have been recorded from the same grating surface for both s-polarized (transverse electric) and p-polarized (transverse magnetic (TM)) incident light, and for in-plane and conical geometries. We test the conical diffraction theory by showing that one set of parameters representing the grating profile and dielectric function of the two media at a constant wavelength may produce theoretically modelled reflectivities which agree with all the experimental data sets. In addition, the surface profile obtained by this optical characterization method is verified by comparison with the profile obtained from an atomic force microscopy (AFM) scan of the surface.

## 2. Experimental details

### 2.1. Experimental geometry

Figure 1 illustrates the experimental geometry and the coordinate system to be considered.

The grating's periodicity provides a mechanism via which the incident radiation may increase or decrease the component of its wave-vector by integer multiples of the grating wave-vector  $\mathbf{k}_g$  ( $k_g = 2\pi/\lambda_g$ ). This gives rise to diffracted orders which become evanescent when their in-plane momentum is increased such that their wave-vector  $k$  becomes greater than the wave vector  $n_d k_0$  of the incident radiation (where  $k_0 = \omega/c = 2\pi/\lambda_0$  and  $n_d = 1.0003$  is the refractive index of air). It is the enhanced wave-vector of these evanescent fields that allows incident radiation to couple to the SPP according to the condition

$$\mathbf{k}_{\text{SPP}} = (n_d k_0 \sin \theta) \mathbf{x} \pm N \mathbf{k}_g. \quad (1)$$

Here  $N$  is an integer,  $\mathbf{k}_{\text{SPP}}$  is the wave-vector of the SPP and  $n_d k_0 \sin \theta$  is the projection of the wave-vector of the incident radiation along the  $x$  axis. If the azimuthal angle is equal to zero, then all the diffracted beams lie in the plane of measurement and equation (1) reduces to a scalar equation.

We can represent the solutions of equation (1) using a reciprocal-space map. A planar metal-dielectric interface may be represented by a single lattice point in  $k$  space, based upon which is a light circle of radius  $n_d k_0 = 2n_d \pi/\lambda_0$ . The area

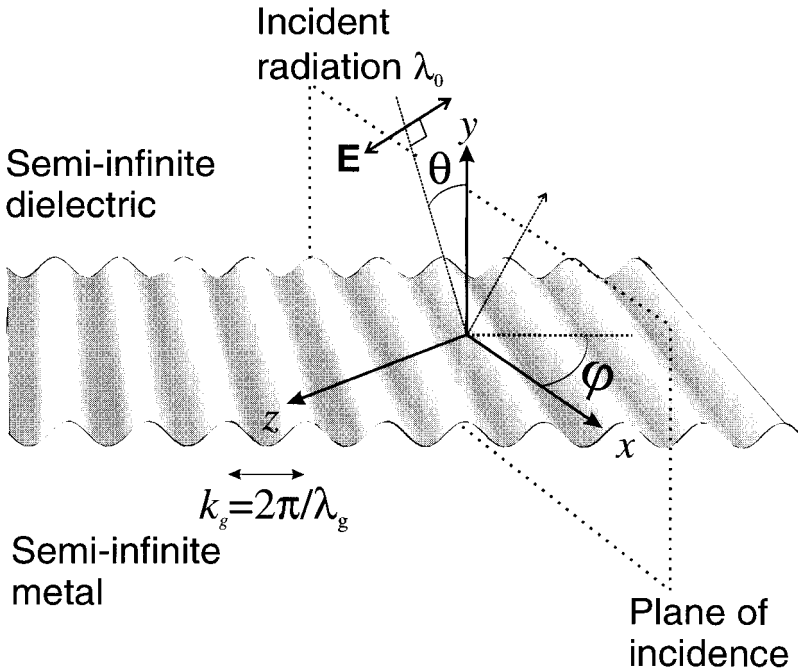


Figure 1. The coordinate system describing the experimental geometry and plane of incidence with respect to the direction of the grating grooves. The direction of the electric field vector  $\mathbf{E}$  is illustrated for the situation when p-polarized (TM) radiation is incident.

bounded by this circle represents the reciprocal space which may be accessed by an incident photon of wave-vector  $n_d k_0$ . The wave-vector associated with a SPP on this planar semi-infinite surface is given by  $k_{\text{SPP}} = k_0 [\varepsilon_d \varepsilon_{\text{mr}} / (\varepsilon_{\text{mr}} + \varepsilon_d)]^{1/2}$  [5], where  $\varepsilon_d (= n_d^2)$  and  $\varepsilon_{\text{mr}}$  are the permittivities of the dielectric and the real part of the metal respectively. This is always higher than that of the incident radiation. Hence the SPP circle has a slightly greater radius than  $n_d k_0$  and therefore, for a planar surface, we may not couple directly to the SPP mode. Of course the corrugation of the metal surface perturbs this SPP wave-vector, but for the amplitude of the grating used in this study (about 30 nm) the effect is small.

The periodic modulation of a diffraction grating scatters the incident radiation by integer multiples of  $k_g$ . This results in a series of diffracted SPP circles about each reciprocal-lattice point. The sections of these diffracted SPP circles that fall within the light circle based upon the origin may now be coupled to by the incident radiation. Figure 2 illustrates the reciprocal-space map for the grating studied in this work. The broken circle about the origin represents the maximum wave-vector available to the incident photon ( $n_d k_0$ ) and the fainter broken circles within this radius represent those that have been scattered by the grating. This illustrates that we may only couple to the SPPs (solid circles) through scattering by  $\pm 1$ ,  $\pm 2$  or  $\pm 3$  grating wave-vectors. The diagram also shows that a photon with wave-vector component  $n_d k_0 \sin \theta$  at an azimuthal angle  $\varphi$  may now couple directly to a SPP. It is also clear that  $\theta$  must vary as  $\varphi$  changes for coupling to be maintained. When

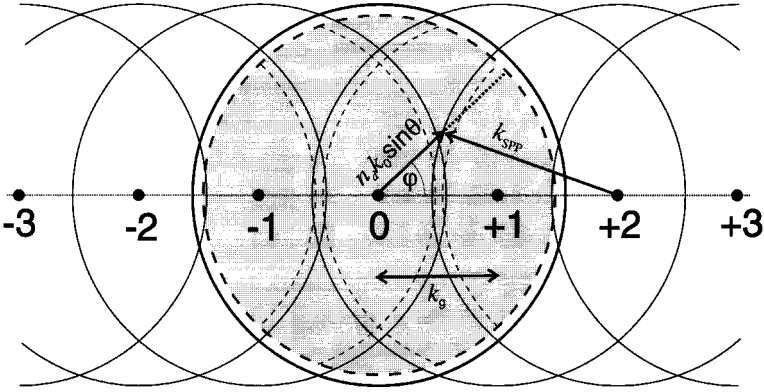


Figure 2. A reciprocal-space map of the grating studied in this work with radiation of wavelength 632.8 nm incident. The numbered points are the lattice points spaced by integer multiples of the grating Bragg vector  $k_g$ . The solid circles centred upon each lattice point of radii  $k_{SPP}$  represent the momentum of the SPP modes associated with that point. The broken circle about the origin of radius  $n_d k_0$  is the incident light circle and the area that it bounds (shaded) contains all the modes accessible to a real photon incident on the grating. The broken arcs of circles within the shaded area represent the portions of scattered light circles that may be accessed by incident photons. The arrow labelled  $n_d k_0 \sin \theta$  indicates the coupling between a photon at incidence angles  $\theta$  and  $\varphi$  to a SPP, via a scattering vector of  $3k_g$ .

$\varphi \neq 0$ , by simple geometry, we find the scalar equivalent of equation (1) is

$$k_{SPP}^2 = n_d^2 k_0^2 \sin^2 \theta + N^2 k_g^2 \pm 2n_d N k_g k_0 \sin \theta \cos \varphi. \quad (2)$$

## 2.2. Experimental procedure

The grating studied in this work was prepared in a silica substrate by standard interferogravaphic techniques [12] which resulted in a grating of pitch  $\lambda_g = 930$  nm. This method of preparation involves the exposure of spin-coated photoresist on a silica disc substrate to two expanded collimated interfering beams followed by its chemical development and the transfer of the profile into the silica by fast-atom etching. This produces a robust diffraction grating, with a surface profile that is somewhat distorted from a pure sinusoid. Subsequent thermal evaporation of an opaque gold layer produces a surface that supports surface plasmons in the visible region of the spectrum. Gold was chosen in preference to silver because its optical properties will not vary over the time scale of the experiment. Incident radiation of wavelength 632.8 nm on a grating of this pitch permits momentum enhancement such that we may couple to six surface plasmon resonances. These are the  $\pm 1$ ,  $\pm 2$  and  $\pm 3$  resonances, where the number and sign refer to the diffracted order that provides the resonant coupling to the SPP.

With conventional studies previously undertaken, the intensity of the specularly reflected beam from the grating is recorded as a function of the polar angle of incidence, generally at fixed wavelength. A schematic diagram illustrating the apparatus required to record such data is shown in figure 3. The grating is rotated about the  $z$  axis and the signal detector moves such that it tracks the specularly reflected beam. If the grating grooves are oriented at the azimuthal angle  $\varphi$

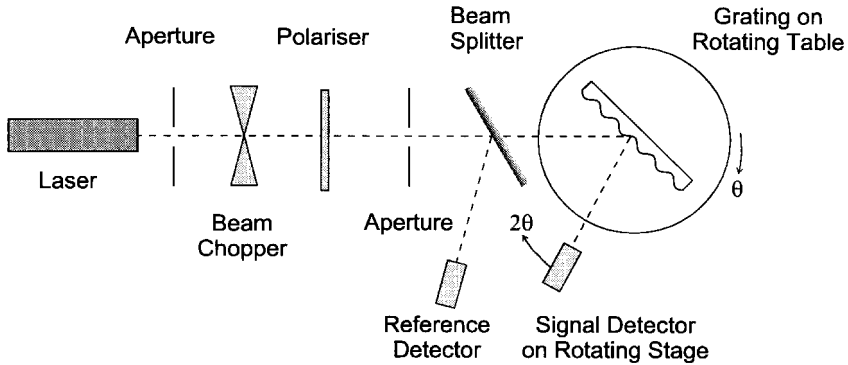


Figure 3. Schematic representation of the experimental set-up used to record polar-angle-dependent reflectivity data from a diffraction grating. In order for the signal detector to track the specularly reflected beam, the signal detector rotates at twice the rate of the grating mounted on the table.

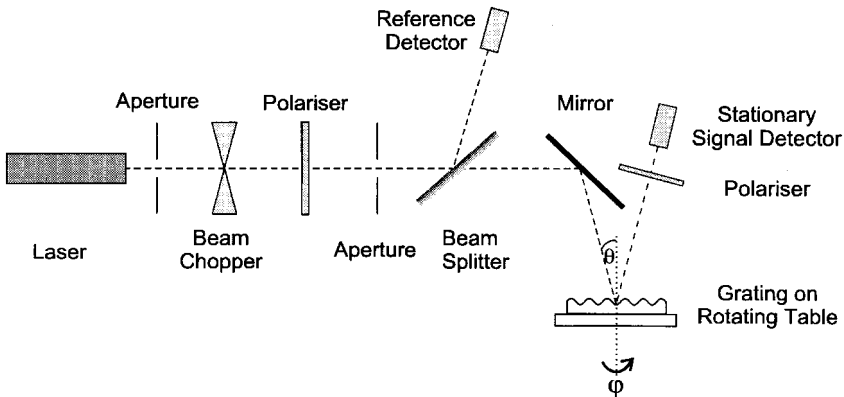


Figure 4. Schematic representation of the experimental set-up used to record azimuthal-angle-dependent reflectivity data from a diffraction grating. The grating is placed on the rotating table with the radiation incident at a fixed polar angle.

depicted in figure 2, the order of features for the 930 nm grating with increasing  $\theta$  would be as follows: the pseudocritical edge associated with the point at which the  $-1$  diffracted order becomes evanescent, SPP ( $-1$ ), SPP ( $+2$ ) and pseudocritical edge ( $+2$ ).

Previous workers have also recorded reflectivity scans as a function of the incident wavelength  $\lambda_0$ . This method has been used to observe directly the SPP dispersion curve both on a planar metal-air interface [13] and on a corrugated interface where an energy gap may open up [14,15]. This method is not particularly suitable for the characterization of metallic gratings since the optical properties of metallic films vary strongly with wavelength, which makes the fitting of data increasingly difficult.

In the present work, the majority of experimental data is recorded as a function of the azimuthal angle  $\phi$ . Figure 4 illustrates the experimental arrangement used to record the azimuthal-angle-dependent data. Unlike the apparatus shown in figure

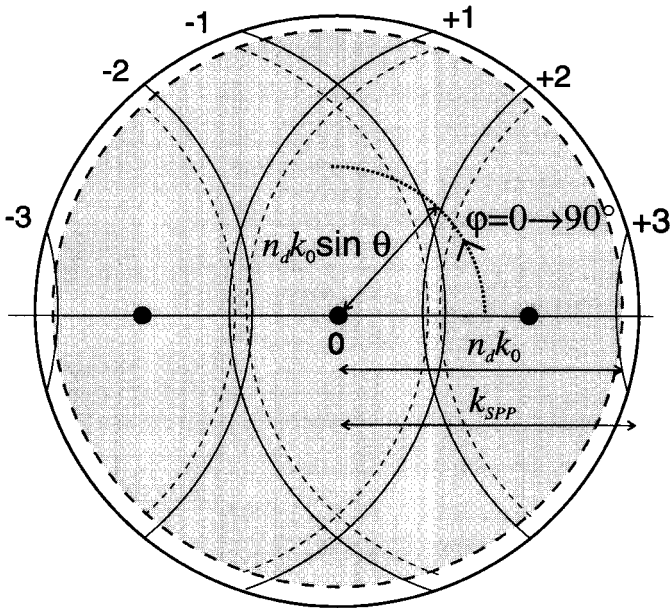


Figure 5. Reciprocal-space map of the grating studied in this work. The dotted arc represents the locus of momentum values traversed during a  $0^\circ$  to  $90^\circ$  azimuthal scan at a constant polar angle.

3 for deriving the polar-angle-dependent data, this method does not require a moving detector. The polar angle  $\theta$  is set using the mirror and the grating placed directly on the rotating table. It is apparent from equation (2) and figure 5 that, if we fix  $\theta$  and vary  $\varphi$ , we shall map out a circle in  $k$  space inside the light circle which will cut SPP and pseudocritical edge arcs that are associated with other diffracted orders. Clearly, from figure 5, if  $\theta$  is too small, then there will be no reflectivity features, and hence a suitable choice of  $\theta$  is required to produce useful data.

In both experimental procedures undertaken in this study, polarizers are used to set the polarization of the incident and detected beams. This allows us to measure the  $R_{pp}$ ,  $R_{ss}$ ,  $R_{sp}$  and  $R_{ps}$  reflectivities, where the subscripts refer to the setting of the incident and detector polarizers respectively. The latter two reflectivities allow us to monitor the polarization conversion reflectivity which is found in the conical mount. It is critically important to ensure that the polarizers are set correctly with respect to the true plane of incidence as p-to-s conversion is acutely sensitive to errors in this alignment.

### 3. Results

In order to deduce the grating profile and optical properties of the metal-dielectric interface, we have matched the reflectivities obtained from a conical version of Chandezon's original differential formalism [9] with those recorded experimentally. The theory involves transforming the optical fields into a non-rectilinear coordinate system in which the interface is mapped on to a plane. Maxwell's equations may be written in this new frame and, by applying the appropriate boundary conditions, which are simplified by the transformation, the

outgoing field amplitudes may be calculated. The theoretical model uses a truncated Fourier sum of sine waves to represent the shape of the interface:

$$A(x) = a_1 \cos(k_g x) + a_2 \cos(2k_g x) + a_3 \cos(3k_g x), \quad (3)$$

where  $a_1$ ,  $a_2$  and  $a_3$  are the fundamental, first and second Fourier harmonics which provide the first-order scattering mechanisms to the  $\pm 1$ ,  $\pm 2$  and  $\pm 3$  SPPs respectively. The series is truncated at the second harmonic because the components that provide the  $4k_g$  and higher scattering vectors are found to be insignificant and have little effect on the reflectivity from the grating used in this study.

Experimental reflectivities were recorded as functions of both the polar and the azimuthal incident angles. Theoretically modelled data were then fitted to the experimental data using an iterative least-squares fitting routine which used the functional form of the grating profile (equation (3)) and the optical permittivity of the metal layer as fitting parameters. The parameters obtained from the optical characterization were  $a_1 = 31.0 \pm 0.4$  nm,  $a_2 = 8.0 \pm 0.5$  nm and  $a_3 = 3.0 \pm 0.4$  nm. The pitch, as defined by the angular position of the pseudocritical edges in the experimental reflectivity data, was calculated to be  $\lambda_g = 930.1 \pm 0.5$  nm with the permittivity of the dielectric (air) set as  $\epsilon_d = n_d^2 = 1.0006$ . The permittivity of the metal (gold) which provided the most accurate fits was  $\epsilon_m = -9.62 + 1.25i$ . Figures 6(a)–(c) show a selection of fits to the experimental azimuthal-angle-dependent reflectivities and, for comparison, figure 6(d) shows a fit to the conventional polar-angle-dependent reflectivity. Figure 6(a) illustrates the polarization conversion that is induced when the grating is in the conical mount. Clearly, the above parameters provide good fits to the experimental data, although the real part of  $\epsilon_m$  is slightly smaller in magnitude than expected for gold at this wavelength ( $\epsilon_m = -10.77 + 1.07i$  [16]).

To confirm that the fitted parameters are indeed a true representation of the grating's profile, AFM was employed to verify the optical characterization technique. The profile was determined by scanning an atomic force microscope stylus over a  $20 \mu\text{m}^2$  area of the grating and then by averaging and Fourier analysing the data. This gave the functional form of the surface as  $a_1 = 30.0 \pm 0.5$  nm,  $a_2 = 8.0 \pm 0.5$  nm and  $a_3 = 2.8 \pm 0.4$  nm. Figure 7 compares this form with the profile obtained by fitting the optical data. The profile recorded by the atomic force microscope stylus shows an apparent reduction in the grating depth. This may be attributed to the fact that the stylus is unable to probe the bottom of the troughs because of its finite width; however, with this relatively shallow grating this is unlikely. More simply the difference is due to a calibration error in the height scale of the atomic force microscope since scaling by a factor of 1.05 gives an almost perfect agreement.

#### 4. Discussion

This work has presented a new experimental technique for the optical characterization of the surface profile of metal diffraction gratings. Figure 6 illustrates that we are able to produce high-quality fits to the experimental data using conical diffraction theory while figure 7 shows convincing agreement between the optical and the AFM-characterized grating profile.

Monitoring the reflectivity data as a function of the azimuthal angle has advantages over the conventional method of polar angle scans, primarily because

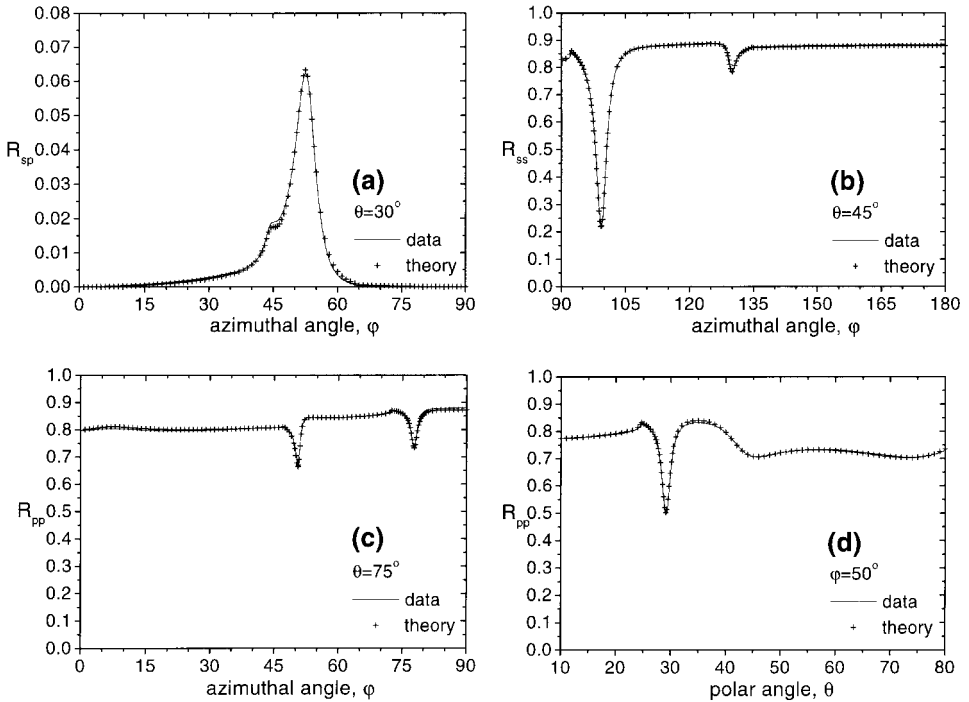


Figure 6. The experimental angle-dependent reflectivities (—) compared with the theoretically modelled reflectivities (+) created from a single set of fitting parameters (a)–(c) illustrate the fits to *azimuthal*-angle-dependent scans at (a)  $\theta = 30^\circ$ , (b)  $\theta = 45^\circ$  and (c)  $\theta = 75^\circ$  for (a)  $R_{sp}$  (polarization conversion), (b)  $R_{ss}$  and (c)  $R_{pp}$  reflectivities. (d) A fit to a *polar*-angle-dependent  $R_{pp}$  reflectivity at a fixed azimuthal angle  $\phi = 50^\circ$ .

the technique does not involve a moving signal detector. This simplifies the apparatus required for such an experiment (figure 4) and eliminates the possibility that experimental errors arise from detector function. In addition, the azimuth scanning method is more favourable for studying gratings at longer incident wavelengths (e.g. microwaves) when the conventional polar angle scans become cumbersome owing to the large area swept out by the signal detector. Furthermore the level of background noise remains constant throughout the experimental scan since only the sample is moving, and hence the use of this technique improves the quality of the resulting fits.

## 5. Conclusions

This work has illustrated that the new technique of experimentally recording the *azimuthal*-angle-dependent reflectivities can be successfully used for the characterization of the surface profile and optical permittivities of metallic diffraction gratings. The experimental procedure to monitor azimuthal-angle-dependent reflectivity data presents a number of advantages over the conventional method of monitoring polar-angle-dependent reflectivities. Particular attention should be drawn to the possible use of this new method in the study of gratings at longer wavelengths.

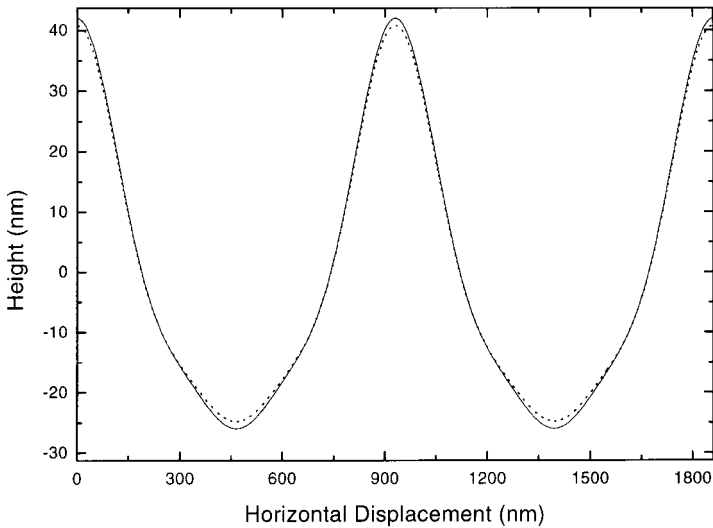


Figure 7. A comparison of the grating profile deduced from the fitting of optical data (—), and the shape determined by AFM measurements (---).

In addition, this work provides a convincing test of conical diffraction theory, producing excellent agreement between the differential formalism of Chandezon and azimuthal-angle-dependent reflectivity experiments. The shape of the surface derived from the fitting process has been shown to be representative of the true profile by comparison with that determined from AFM measurements.

### Acknowledgments

The authors would like to acknowledge the financial support of the Defence Evaluation and Research Agency (DERA), Farnborough, and wish to thank Alex Smout (DERA, Malvern) for his contribution to the AFM study.

### References

- [1] WOOD, R. W., 1902, *Phil. Mag.*, **4**, 396.
- [2] FANO, U., 1941, *J. opt. Soc. Am.*, **31**, 213.
- [3] TENG, Y. Y., and STERN, E. A., 1967, *Phys. Rev. Lett.*, **19**, 511.
- [4] BURSTEIN, E., CHEN, W. P., CHEN, Y. J., and HARSTEIN, A., 1974, *J. vac. Sci. Technol.*, **11**, 1004.
- [5] RÄETHER, H., 1988, *Surface Plasmons on Smooth and Rough Surfaces and on Gratings* (Berlin: Springer).
- [6] CHANDEZON, J., DUPUIS, M. T., CORNET, G., and MAYSTRE, D., 1982, *J. opt. Soc. Am.*, **72**, 839.
- [7] WOOD, E. L., SAMBLES, J. R., COTTER, N. P., and KITSON, S. C., 1995, *J. mod. Optics*, **42**, 1343.
- [8] NASH, D. J., and SAMBLES, J. R., 1996, *J. mod. Optics*, **43**, 81.
- [9] ELSTON, S. J., BRYAN-BROWN, G. P., and SAMBLES, J. R., 1991, *Phys. Rev. B*, **72**, 6393.
- [10] BRYAN-BROWN, G. P., and SAMBLES, J. R., 1990, *J. mod. Optics*, **37**, 1227.
- [11] WATTS, R. A., SAMBLES, J. R., and HARRIS, J. B., 1997, *Optics Commun.*, **135**, 189.
- [12] HUTLEY, M. C., 1982, *Diffraction Gratings* (London: Academic Press).

- [13] SWALEN, J. D., GORDON, J. G., II, PHILPOTT, M. R., BRILLANTE, A., POCKRAND, I., and SANTO, R., 1980, *Am. J. Phys.*, **48**, 669.
- [14] WEBER, M. G., and MILLS, D. L., 1986, *Phys. Rev. B*, **34**, 2893.
- [15] KITSON, S. C., BARNES, W. L., SAMBLES, J. R., and COTTER, N. P. K., 1996, *J. mod. Optics*, **43**, 573.
- [16] BRYAN-BROWN, G. P., ELSTON, S. J., and SAMBLES, J. R., 1991, *J. mod. Optics*, **38**, 1181.